

Effect of Strain on the Energy Band Gaps of (13,0) and (15,0) Carbon Nanotubes

G. Dereli, N. Vardar and O. Eyecioğlu

Department of Physics, Yildiz Technical University, İstanbul, Turkey
gdereli@yildiz.edu.tr, necativardar@gmail.com, oyeci@yildiz.edu.tr

ABSTRACT

The electronic energy band gap is a basic property of all semiconductors since it is responsible for the electrical transport and optical properties. Control of the size of the energy band gap is important in optimizing electronic devices. In this study, we have shown that the application of tensile strain modifies the size of the band gaps in semiconducting Single Walled Carbon Nanotubes (SWCNTs) and opens a band gap in metallic SWCNTs. We simulated (13,0) and (15,0) SWCNTs under various compressive and tensile strain at 300K. Pristine (13,0) SWCNT is a semiconductor with a band gap of 0.44 eV and (15,0) SWCNT is metallic. The strain was applied as both compression and stretching along the z -direction. The density of states are obtained in real space using a parallel Order N, Tight Binding Molecular Dynamic (O(N) TBMD) simulation code designed by Dereli *et. al.* [1-3]. The energy band gaps of (13,0) and (15,0) SWCNTs demonstrate different behaviors with the presence of strain. For (13,0) tube, energy band gap decreases with negative strain values (compression) and the onset of semiconductor-metal transition occurs at a negative strain value of %8. For (15,0) SWCNT, application of positive and negative strains opens up the band gap causing metal - semiconductor transitions.

Keywords: Single-walled carbon nanotubes, Order-N Tight-Binding Molecular Dynamics simulations, strain, electronic energy band gap modifications.

1 INTRODUCTION

Single Walled Carbon Nanotubes (SWCNTs) display a variety of electronic structures depending on their chirality. The structure of a SWCNT is specified by a chiral vector ($\vec{C}_h = (n, m)$). Depending on the chirality vector, SWCNTs are classified into three types, namely, armchair (n, n), zigzag ($n, 0$) and chiral (n, m). The armchair SWCNTs are always metallic, and the zigzag SWCNTs are metallic only when n is a multiple of 3.

Control of the size of the energy band gap is important in optimizing such devices as p-n junctions, transistors, photodiodes and laser works. In the present work, we have shown that the presence of positive and negative strain modifies the size of the energy band gaps in

semiconducting SWCNTs and opens a band gap in metallic SWCNTs.

We demonstrated the modification of the electronic band gap with strain on (13,0) and (15,0) SWCNTs. At 300K and zero strain, (13,0) SWCNT is a semiconductor with a band gap of 0.44 eV and (15,0) SWCNT is metallic. The strain was applied as both compression and tension along the z direction. The results are obtained using a parallel Order N, Tight Binding Molecular Dynamic (O(N) TBMD) simulation code designed by Dereli *et. al.* [1-3]. This code is used in SWCNTs simulations successfully and the details of the technique can be followed in [4-6].

O(N) TBMD calculates the band structure energy in real space and makes the approximation that only the local environment contributes to the bonding, and hence the band energy of each atom. In this case, the run time would be linearly scaled with respect to the number of atoms.

We simulated (13,0) and (15,0) SWCNTs under various compressive and tensile strain values. Positive strain values correspond to tensile and the negative strain values to compressive strain. Strain values are chosen to stay in the plastic region for these SWCNTs. Total energy and Fermi energy levels are obtained as functions of strain. Band gap is calculated from the behavior of electronic density of states near the Fermi energy level for each strain values.

2 METHOD

Our simulations are performed using Order N, Tight Binding Molecular Dynamic (O(N)-TBMD) simulation technique for the canonical (NVT) ensemble. Inter-atomic forces needed to move atoms are calculated from TBMD Hamiltonian by means of the Hellman-Feynman theorem. The many body Hamiltonian (H_{tot}) is reduced to Hamiltonian (h) of one electron moving in the average field due to other electron and ion cores:

$$H_{tot} = K_i + K_e + U_{ee} + U_{ie} + U_{ii} \quad (1)$$

$$h = K + U_{ie} + U_{ee} \quad (2)$$

The corresponding Schrödinger's equation is written as:

$$h|\psi_n\rangle = \varepsilon_n|\psi_n\rangle \quad (3)$$

where $|\psi_n\rangle$ are eigenstates corresponding to the eigenvalues ε_n . In TB formalism, $|\psi_n\rangle$ are taken as linear combinations of atomic orbitals $|\phi_{l\alpha}\rangle$ (l : quantum number index, α : labels the ions)

$$|\psi_n\rangle = \sum_{l\alpha} C_{l\alpha}^n |\phi_{l\alpha}\rangle \quad (4)$$

Since the $|\phi_{l\alpha}\rangle$ basis set is not orthogonal, one may use instead the orthogonal set of atomic orbitals known as Löwdin orbitals $|\varphi_{l\alpha}\rangle$ 'n terms of which the secular equation becomes

$$\sum_{l'\beta} (\langle \varphi_{l'\beta} | h | \varphi_{l\alpha} \rangle - \varepsilon_n \delta_{ll'} \delta_{\alpha\beta}) C_{l'\beta}^n = 0. \quad (5)$$

To solve this secular equation with as small number of TB parameters as possible, some approximations are made [7]: (i) Minimal basis set is used in secular equation. In this study we use sp^3 basis set for SWCNTs. (ii) the hopping integrals corresponding to interatomic distance larger than a suitable cutoff are not considered. (iii) only two-center integrals are taken into account.

The key objects of the secular equation are the matrix elements $\langle \varphi_{l'\beta} | h | \varphi_{l\alpha} \rangle$ known as hopping integrals of one electron Hamiltonian. The equilibrium hopping integrals $\langle \varphi_{l'\beta} | h | \varphi_{l\alpha} \rangle = h_{ll'}^{(0)}$ are generalized as

$$h_{ll'}(r_{\alpha\beta}) = h_{ll'}^{(0)} f_{ll'}(r_{\alpha\beta}) \quad (6)$$

where $f_{ll'}(r_{\alpha\beta})$ is known as the scaling function for atoms which are not in their equilibrium positions .

The solution of the secular equation determines the single electron eigenvalues ε_n . The total energy of a system of ion cores and valence electron is obtained as

$$U_{tot} = 2 \sum_n \varepsilon_n f(\varepsilon_n, T) + U_{ii} - U_{ee} = U_{bs} + U_{rep} \quad (7)$$

where $f(\varepsilon_n, T)$ is the Fermi-Dirac distribution function, $-U_{ee}$ corrects the double counting of the electron-electron interaction in the first term. The sum of all the single particle energies is commonly called the band structure energy and denoted by

$$U_{bs} = 2 \sum_n \varepsilon_n f(\varepsilon_n, T). \quad (8)$$

The factor of 2 in the first term comes from spin degeneracy. The effective repulsive potential is expressed as a sum of suitable short ranged two-body potentials [8]

$$U_{rep} = U_{ii} - U_{ee} = \sum_{\alpha, \beta > \alpha} \Phi(r_{\alpha\beta}) \quad (9)$$

where $\Phi(r_{\alpha\beta})$ is a pairwise potential between atoms α and β and $r_{\alpha\beta}$ is a pairwise distance between atoms. The functional form suggested by Goodwin, Skinner and Pettifor is used for pair wise potentials in [8,9] so that the TBMD Hamiltonian and corresponding forces are expressed as:

$$H_{TBMD} = \sum_{\alpha} \frac{p_{\alpha}^2}{2m_{\alpha}} + \sum_n \varepsilon_n f(\varepsilon_n, T) + U_{rep} \quad (10)$$

$$\vec{F}_{tot, \alpha} = - \sum_n \left\langle \psi_n \left| \frac{\partial H}{\partial \vec{r}_{\alpha}} \right| \psi_n \right\rangle f(\varepsilon_n, T) - \frac{\partial U_{rep}}{\partial \vec{r}_{\alpha}}. \quad (11)$$

The repulsive force term can be computed analytically since repulsive potential U_{rep} is known as a function of the interatomic distances:

$$F_{rep} = - \frac{\partial U_{rep}}{\partial r_{\alpha}} = - \frac{\partial}{\partial r} \sum_{\alpha} f(\sum_j \phi(r_{\alpha\beta})). \quad (12)$$

Attractive force can be computed only numerically through Hellman-Feynman theorem. Hellman-Feynman contribution to the net force is given by

$$\sum_n \langle \psi_n | \frac{\partial H}{\partial \vec{r}_{\alpha}} | \psi_n \rangle f(\varepsilon_n, T) = \sum_n f(\varepsilon_n, T) \sum_{l\alpha} \sum_{l'\beta} C_{l\alpha}^n \frac{\partial H_{ll'\alpha\beta}(r_{\alpha\beta})}{\partial \vec{r}_{\alpha}} C_{l'\beta}^n. \quad (13)$$

In order to determine the band structure energy and Hellman-Feynman forces, we need to know the full spectrum of eigenvalues ε_n and the corresponding eigenvectors $C_{l\alpha}^n$. So we must diagonalize the TBMD Hamiltonian matrix at every time step of the simulation. The standard diagonalization of the TB matrix of dimension $nN \times nN$ (N is the number of the atoms in the system and n is the number of valance electrons per atom) requires computation time that scales as $O(N^3)$ and dominates the overall computational workload of the TBMD simulations. On the other hand by using an $O(N)$ algorithm, it is possible to reduce the scale of the computation time from N^3 to N . The recent $O(N)$ methods solve for the band energy in real space and make the approximation that only local environment contributes to the bonding and hence bond energy of each atom[10]. One of the $O(N)$ methods commonly used to carry out quantum calculations is the divide and conquer (DAC) approach [11]. The key idea of this approach is to provide a description of a large system in terms of contributions from subsystems. The system is split into sub systems and each subsystem is solved independently. Each subsystem comes with its own Hamiltonian matrix, constructed relative to the corresponding buffer. The effect of the buffer size on $O(N)$ TBMD is very important. We calculated the buffer size as 4.8A for a (15,0) SWCNT and 4.6 A for a (13,0) SWCNT. The cubodial box size is taken as the distance between two cross-sectional layers along the uniaxial direction (1.229A) and periodic boundary condition (PBC) is applied along the z direction only. Interaction cut off distance is chosen as 2.6 A. The simulations are performed using parallel $O(N)$ TBMD simulation method on distributed memory system consisting of a Linux cluster with 16 PC's. The simulation code was written in Fortran77 programming language by G. Dereli et. al. [1-3]. Dynamic memory allocation is used for all dynamic variables. Code is designed according to SIMD taxonomy.

3 RESULTS AND DISCUSSION

Snapshots of the simulated SWCNTs can be seen in Figure 1. Strain was applied along the axial (z) direction and SWCNTs are allowed to relax along the other directions (x and y). The axial strain is obtained from $\varepsilon = (l - l_0)/l_0$ where l_0 is the equilibrium length in the axial direction for unstrained SWCNT and the l is the corresponding length in the strained SWCNT. Positive strain values correspond to tension and negative strain values to compression. Simulations are performed at room temperature and the periodic boundary condition is applied along the z direction. Velocity Verlet algorithm along with the canonical ensemble molecular dynamics (NVT) is used. Our simulation procedure is as follows:

(i) The tube is simulated at 300K for a 3000 MD steps of run time with a time step of 1 fs. This eliminates the possibility of the system to be trapped in a metastable state. We wait for the total energy to reach the equilibrium state.

(ii) Next, uniaxial strain is applied to the tubes. We further simulated the deformed tube structure (the under uniaxial strain) for another 2000 MD steps. Figure 2, shows the variation of the total energy of strained SWCNTs during MD simulations for the several strain values corresponding to compression and tension. First 3000 MD steps show equilibrium of the unstrained SWCNTs and the next 2000 MD steps show the variation of the total energy of the SWCNTs during the simulations under applied strain. In the figure, it is seen that (13,0) and (15,0) SWCNTs are able to sustain their structural stability under applied strain in the elastic limit. In Figure 3, we present the change in the density of states of (13,0) and (15,0) SWCNTs under strain. Energy band gap is calculated from the behavior of eDOS around the fermi level. Strain is applied in the plastic region of $\% - 8 \leq \varepsilon \leq \%8$.

Effect of uniaxial strain on the energy band gaps of (13,0) and (15,0) SWCNTs are given in Figure 4. The energy band gaps of (13,0) and (15,0) SWCNTs respond differently to the presence of uniaxial strain. At zero strain (13,0) SWCNT is a semiconductor with an energy band gap of 0.44 eV. Application of negative strains closes the band gap causing semiconductor-metal transitions. For (13,0) SWCNT, energy band gap decreases with negative strain (compression) and the onset of semiconductor-metal transition occurs at the negative strain value of $\%8$. On the other hand, positive strain increases the energy band gap of (13,0)SWCNT. For (15,0) SWCNT energy band gap increases both with the presence of positive and negative strain. Applications of positive and negative strains open up the band gap causing metal - semiconductor transitions in (15,0) SWCNT.

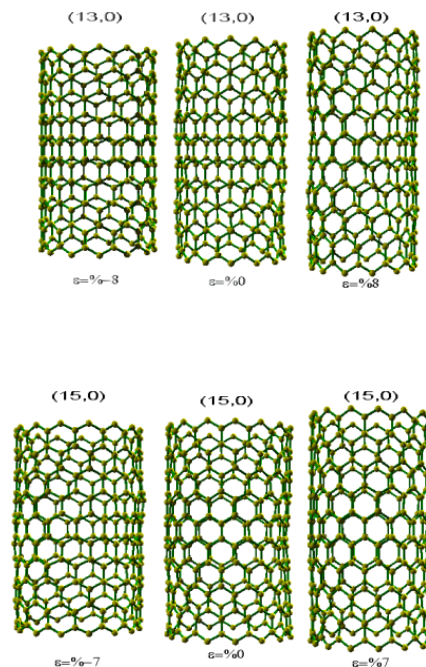


Figure 1: Snapshots of simulated SWCNTs

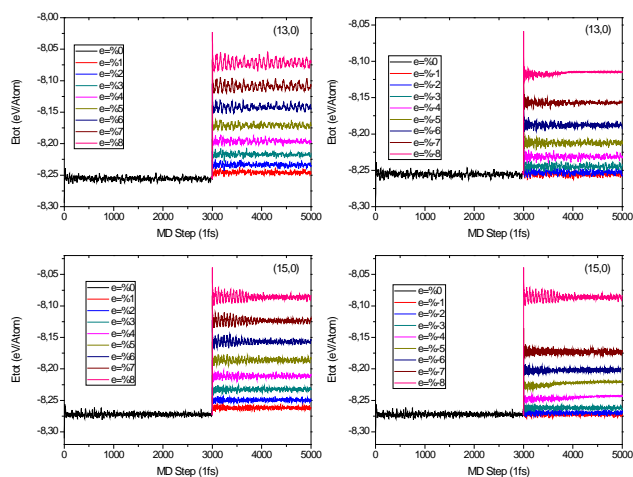


Figure 2: Variations of total energy with strain

4 CONCLUSION

In summary, the electronic structures of deformed (13,0) and (15,0) SWCNTs under strain are simulated in real space using Order N Tight-Binding Molecular Dynamics simulation technique. Our studies show that the energy band gaps of these zig-zag SWCNTs respond differently to the presence of uniaxial strain. The zigzag SWCNTs are generally semiconducting and they are metallic only when n is a multiple of 3. (15,0) SWCNT is a zig-zag nanotube and the application of external strain brings it back to semiconducting state. For (13,0) tube, electronic band gap decreases with compression and the onset of semiconductor-metal transition occurs at negative strain value of %8. What determines if a SWCNT is metallic or not is whether the quantized components of the electronic wave vectors along the circumferential direction intersects or not the graphene's Fermi surface during folding. For example, $(n,0)$ zigzag SWCNTs are metallic only when n is a multiple of three, because only in this case do the quantized k vectors cross the vertices of the hexagonal Brillouin zone of the graphene sheet. Our study shows the potential of a tunable energy band gap of SWCNTs through the application of positive and negative uniaxial strain. The findings of this paper will be helpful in the construction of SWCNT based nano-electronic devices.

The research reported here is supported through the Yildiz Technical University Research Fund Projects YTU 29-01-01-YL02 and YTU 24-01-01-04. The simulations are performed at the Carbon Nanotubes Simulation Laboratory, Department of Physics, Yildiz Technical University, Istanbul, Turkey

http://www.yildiz.edu.tr/~gdereli/lab_homepage/index.html

REFERENCES

- [1]G. Dereli, C. Özdoğan, Phys. Rev. B67, 0354416, 2003.
- [2]G. Dereli, C. Özdoğan, Phys. Rev. B67, 0354415, 2003.
- [3]C. Özdoğan, G. Dereli, T. Çağın, Comput. Phys. Commun., 148, 188-205, 2002.
- [4]G. Dereli, B.Süngü, Phys. Rev. B75, 184104, 2007.
- [5]G. Dereli, B.Süngü, C. Özdoğan, Nanotechnology 18, 245704, 2007.
- [6]B.Onat, M.Konuk, S.Durukanoglu and G. Dereli, Nanotechnology 20 ,075707, 2009.
- [7]L.Colombo, Comput. Mater. Sci., 12, 278, 1998.
- [8]C. H. Xu. C. Z. Wang, C. T. Chang. K. M. Ho, J. Phys.: Cond. Matt. 4, 6047, 1992.
- [9]L. Goodwin, A. J. Skinner and D. G. Pettifor, Europhys. Lett. 9, 701, 1989.
- [10]P. Ordejon, Comput. Mater. Sci., 12, 157, 1998.
- [11]W. Yang, Phys. Rev. Lett. 66, 1438, 1991.

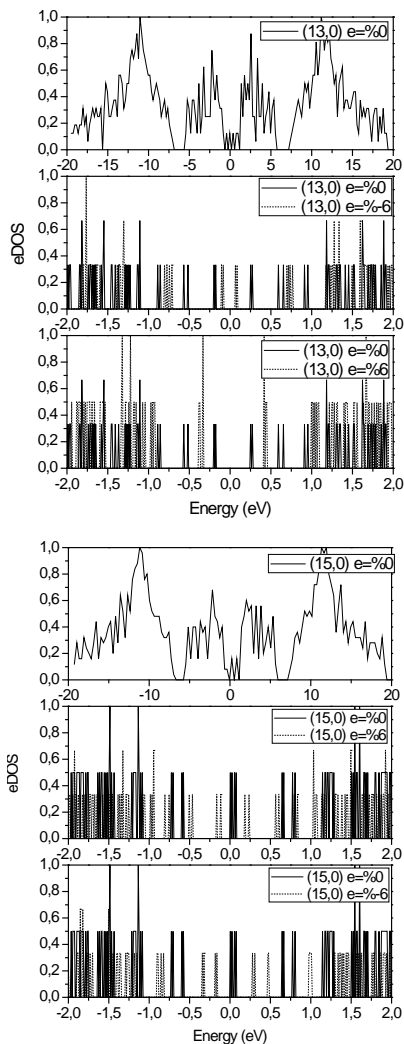


Figure 3: Density of states of (13,0) and (15,0) SWCNTs under strain

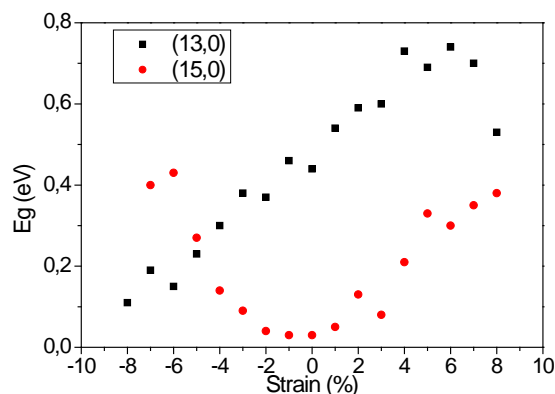


Figure 4: Variations of energy band gaps with strain